Capturing the HI 21 cm Signal in Ground-Based Observations Amidst Diverse Systematic Influences

Abhirup Datta
Indian Institute of Technology Indore, India

Anshuman Tripathi, Samit Kumar Pal, Rashmi Sagar (IITI)

Cosmic Dawn at High Latitudes Conference

Contributors

Anshuman Tripathi
(Final Year PhD Student)

Samit K. Pal
(Fourth Year PhD Student)

Rashmi Sagar
(Fourth Year PhD Student)

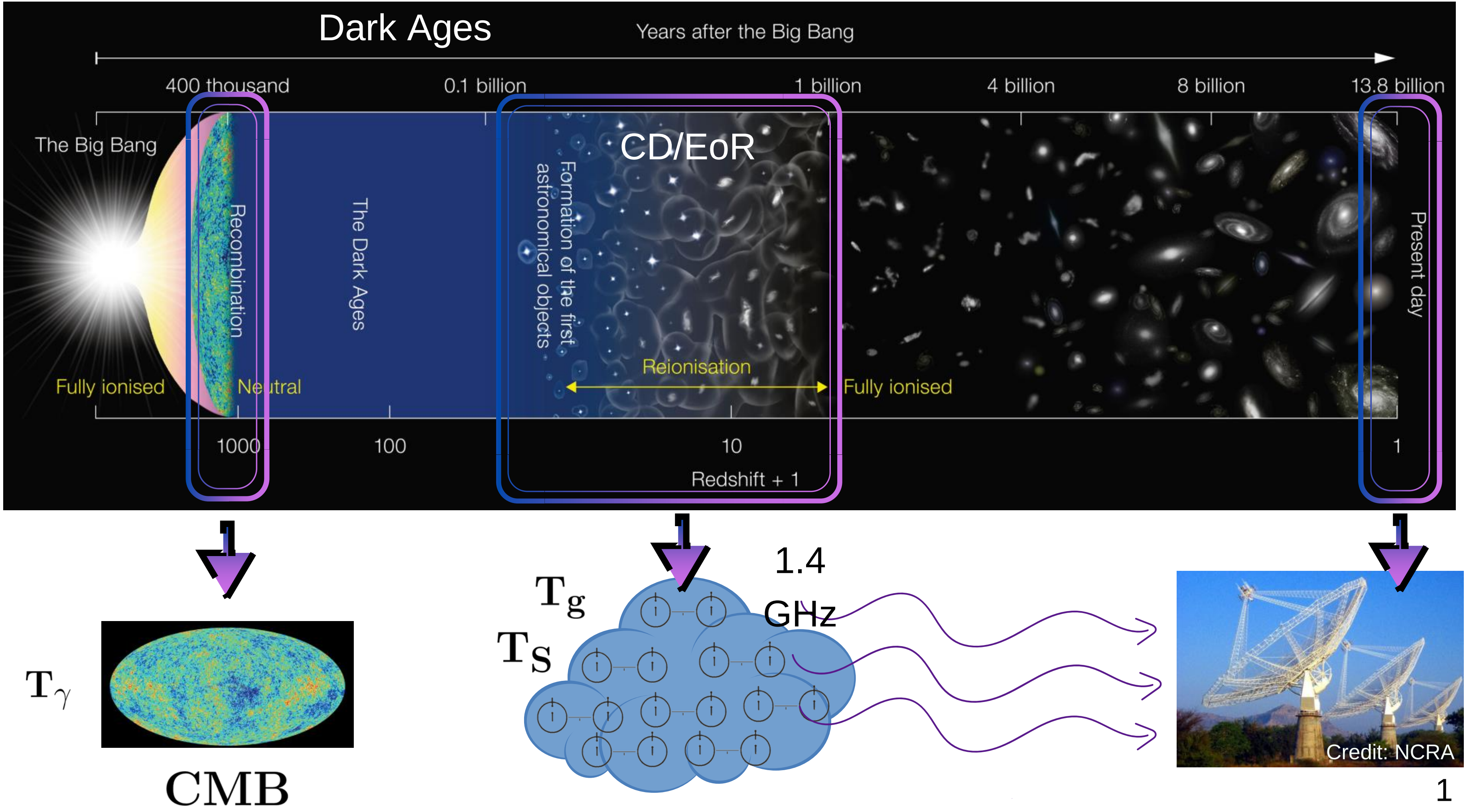
Dark Ages
Years after the Big Bang
400 thousand
0.1 billion
1 billion
4 billion
8 billion
13.8 billion
The Big Bang
Recombination
The Dark Ages
Formation of the first astronomical objects
CD/EoR
Present day
Fully ionised
Neutral
Reionisation
Fully ionised
1000
100
10
1
Redshift + 1
T_γ
CMB
T_g
T_S
1.4 GHz
Credit: NCRA

Biggest Challenge : Foregrounds

Dominant (~ 70% Contribution)

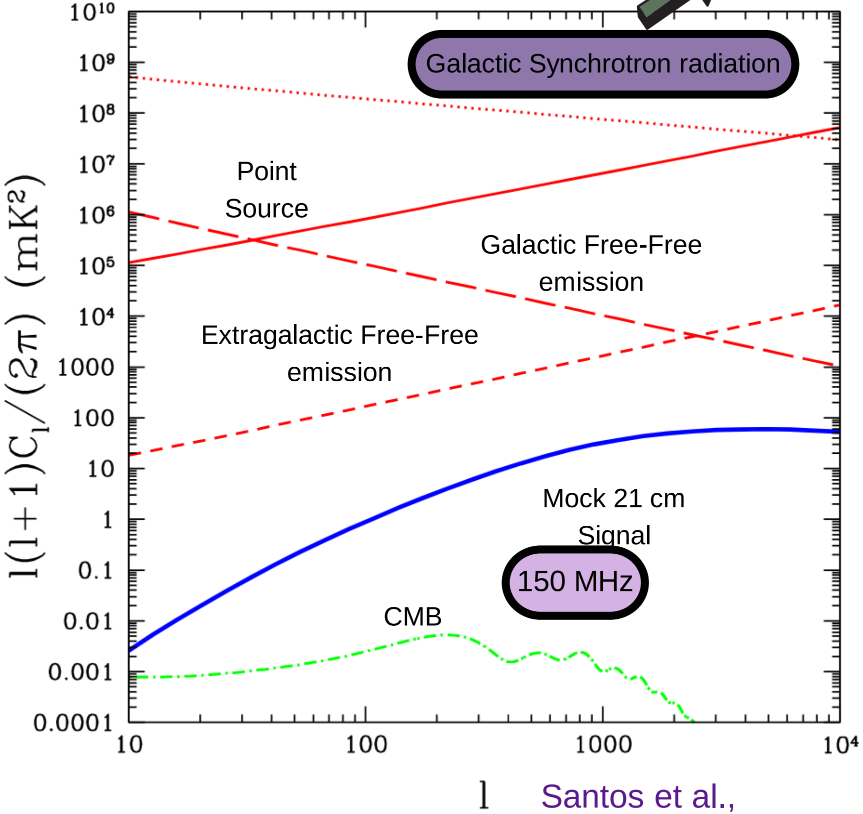

Santos et al.,

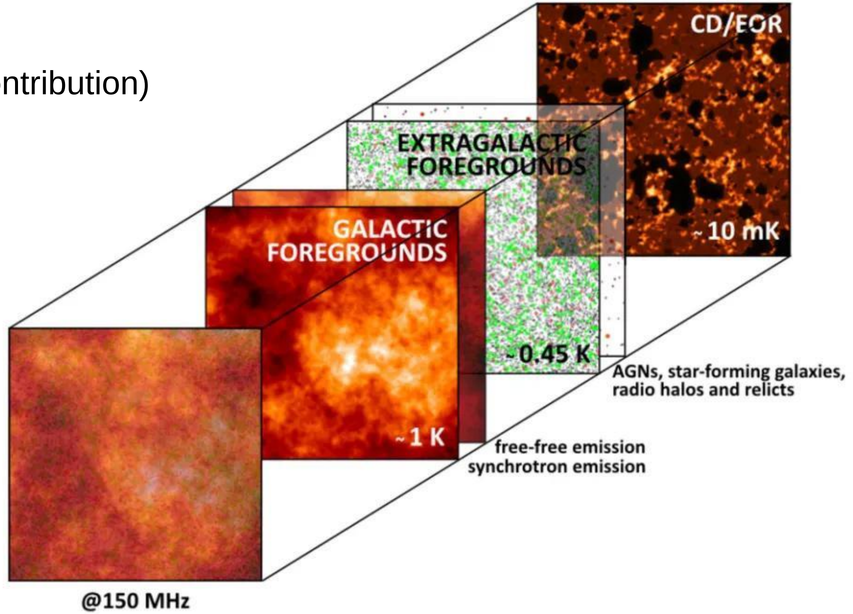

Signal + Foreground at 150MHz

Chapman et al., 2019

A challenging experiment

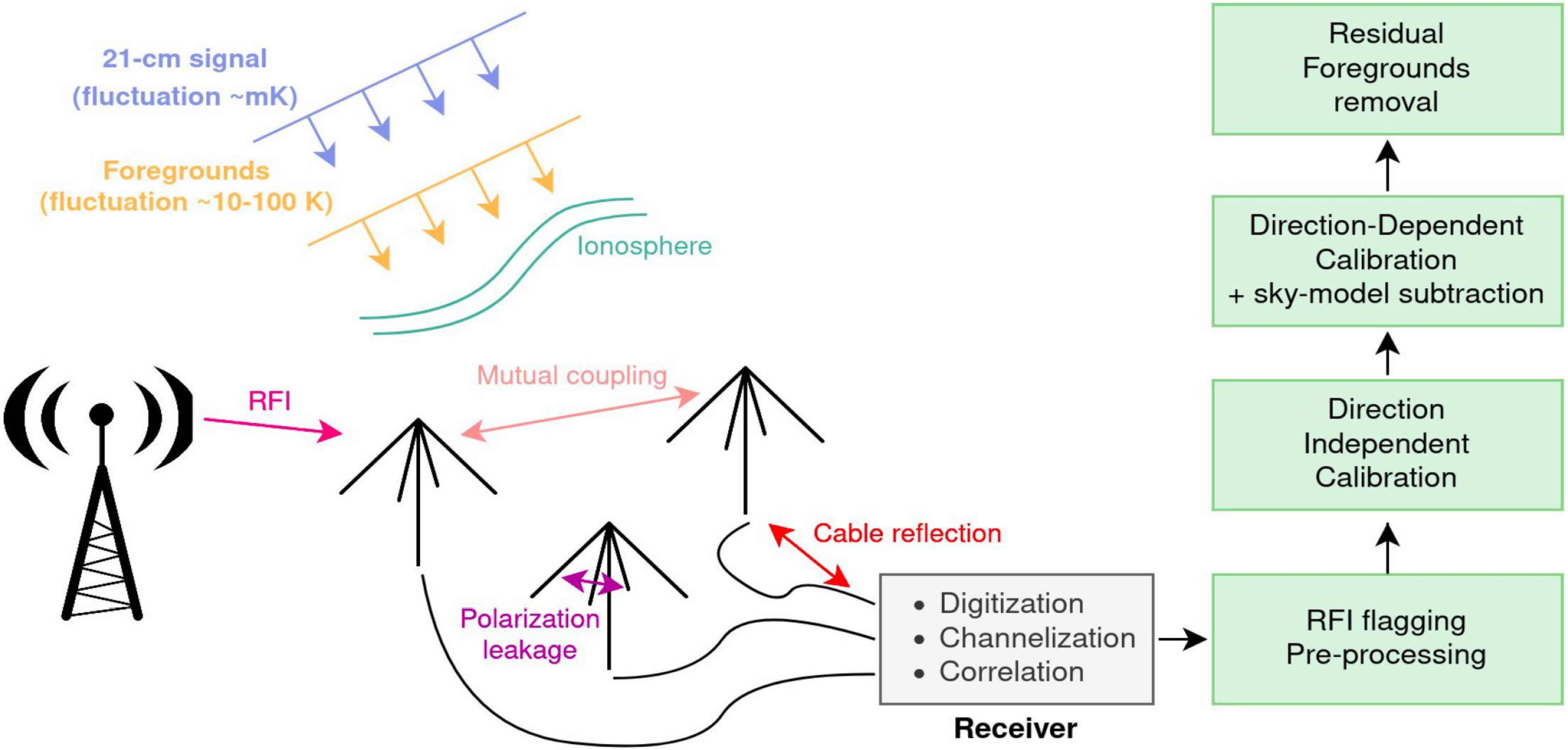

Courtesy: F. Mertens

Motivation:

- ELAIS-N1 field is at high galactic latitudes.
- Characterization of diffuse radio background at 183MHz with uGMRT.

Previous work in ELAIS N1 field :

- Performed direction-independent calibration in Band-3.
- The angular power spectrum using TGE.
- Upper limit in Band-3.

NEW:

- Direction-Dependent calibration in Band-2.
- Power spectra estimation using Image-based estimator.
- Image-based estimator is promising tool to retrieve low multipoles at low-frequency.

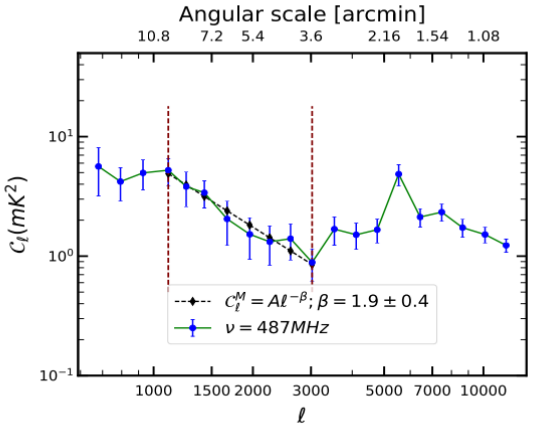

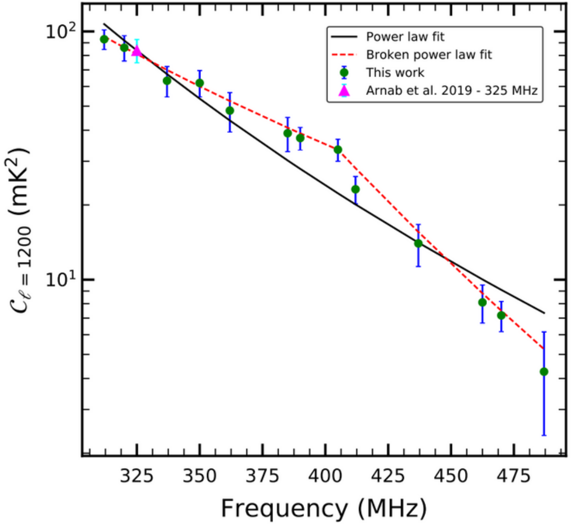

Chakraborty et al., 2019

Observations from uGMRT near 150 MHz

Observational INFO

RFI & Noise

Data Observation from GMRT

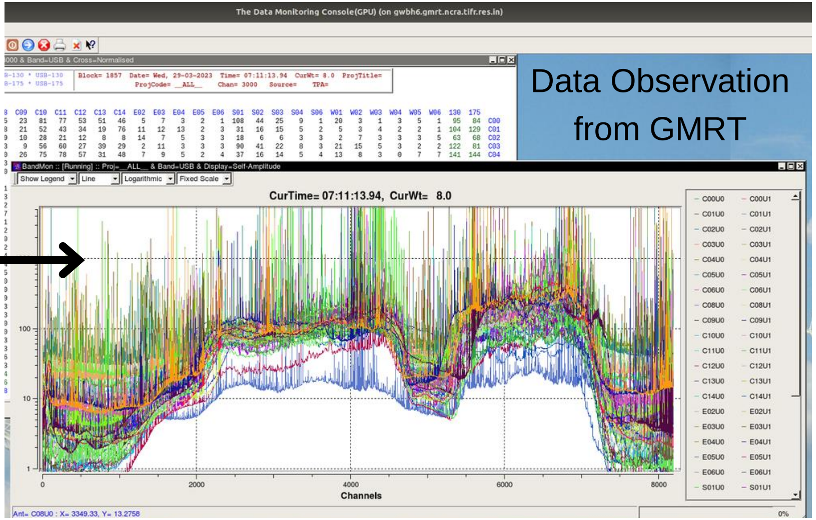

Total Observation Time	32 hours
Frequency	183MHz
Bandwidth	120 - 250 MHz
Integration Time	5.37sec
Number of Channels	8192
Frequency Resolution	24 KHz
Target field $(\alpha, \delta)_{2000}$	$(16^h 10^m 1^s, +54°30'36")$
Working Antennas	27

Pointing centres	$13^h 31^m 08^s$ $+30^d 30^m 32^s$	(3C286)
	$15^h 49^m 17^s$ $+50^d 38^m 05^s$	(J1549+506)
	$16^h 10^m 01^s$ $+54^d 30^m 36^s$	(ELAIS N1)
	$01^h 37^m 41^s$ $+33^d 09^m 35^s$	(3C48)

UV - coverage

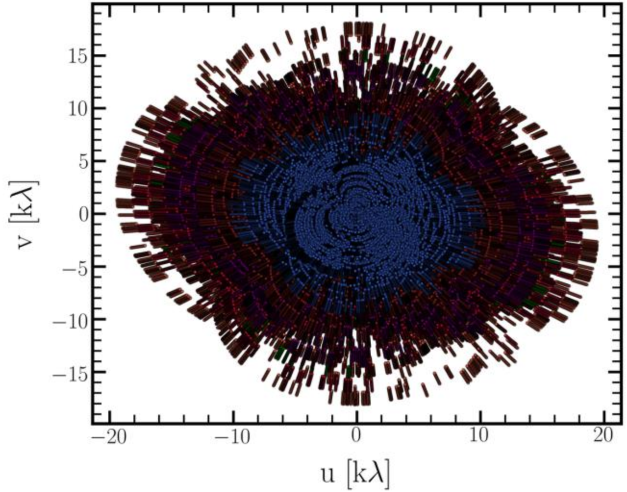

Sagar et al., (In prep.)

Direction-Dependent Calibration : SPAM

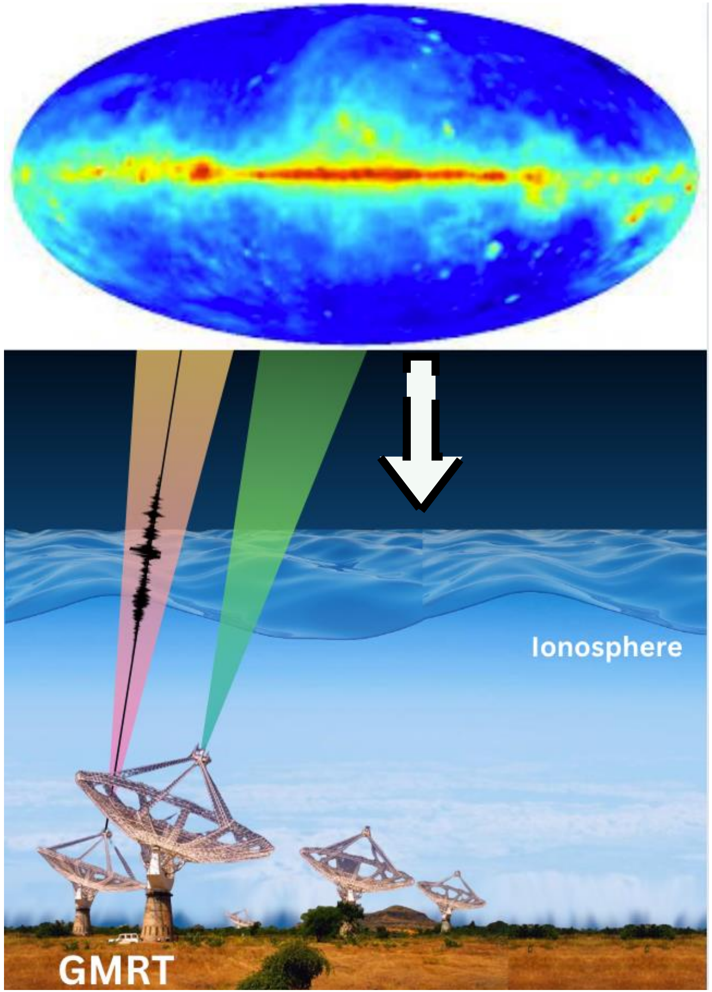

- SPAM : Pre-processing, Main pipeline.
- Solves ionospheric phases & corrects ionospheric phase errors.
- Correction in ionospheric delay improves the background noise & flux-scale accuracy.

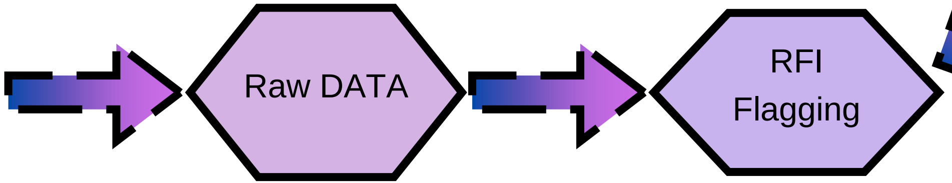

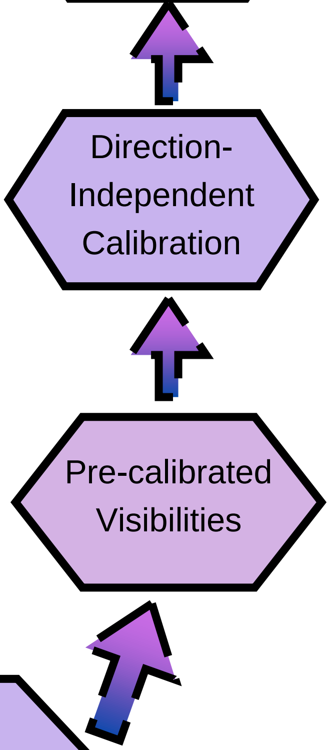

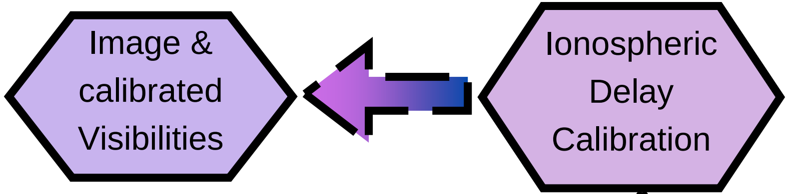

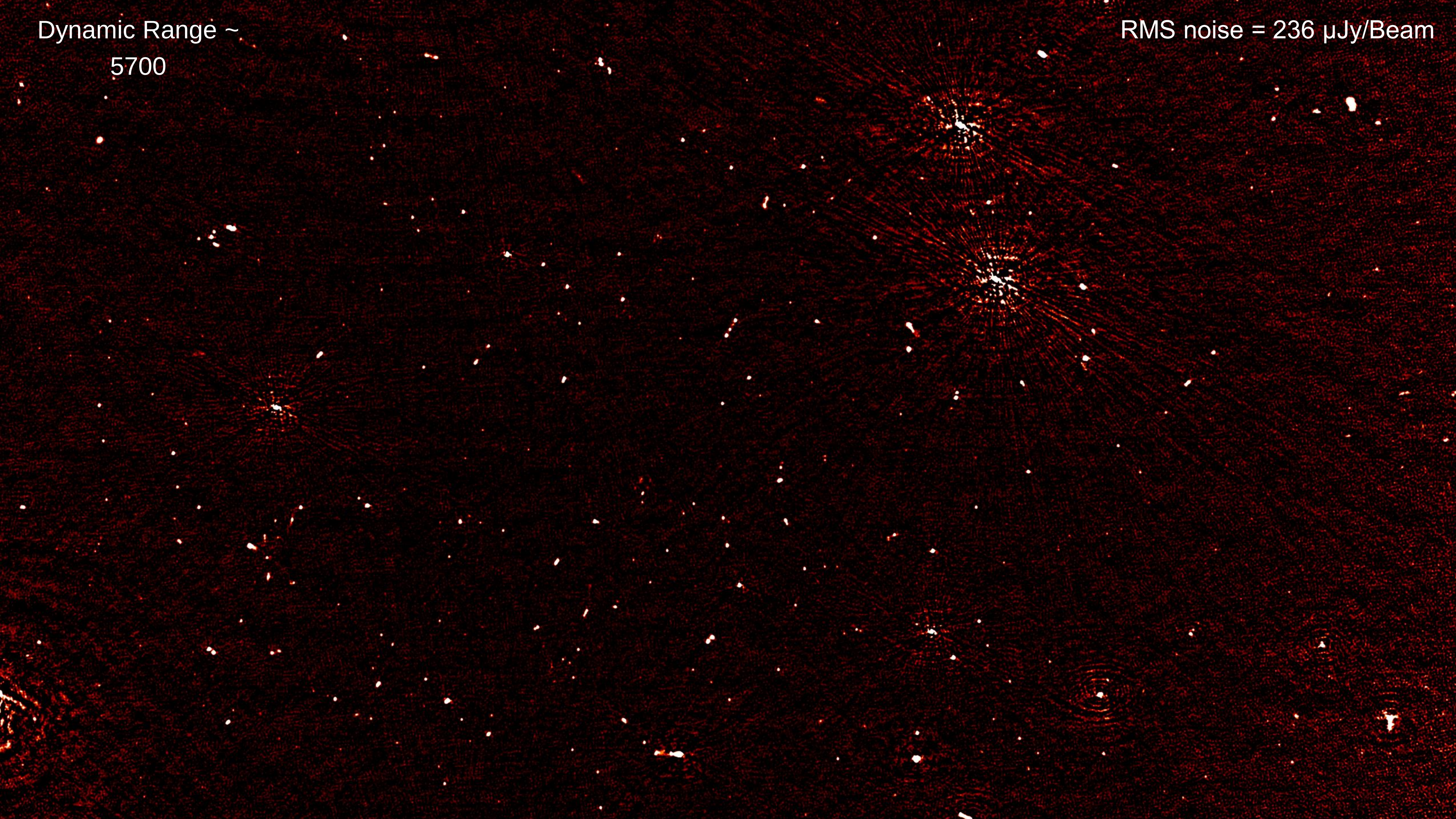
Dynamic Range ~
5700
RMS noise = 236 μJy/Beam

Comparison with other catalog: Source catalog reliability

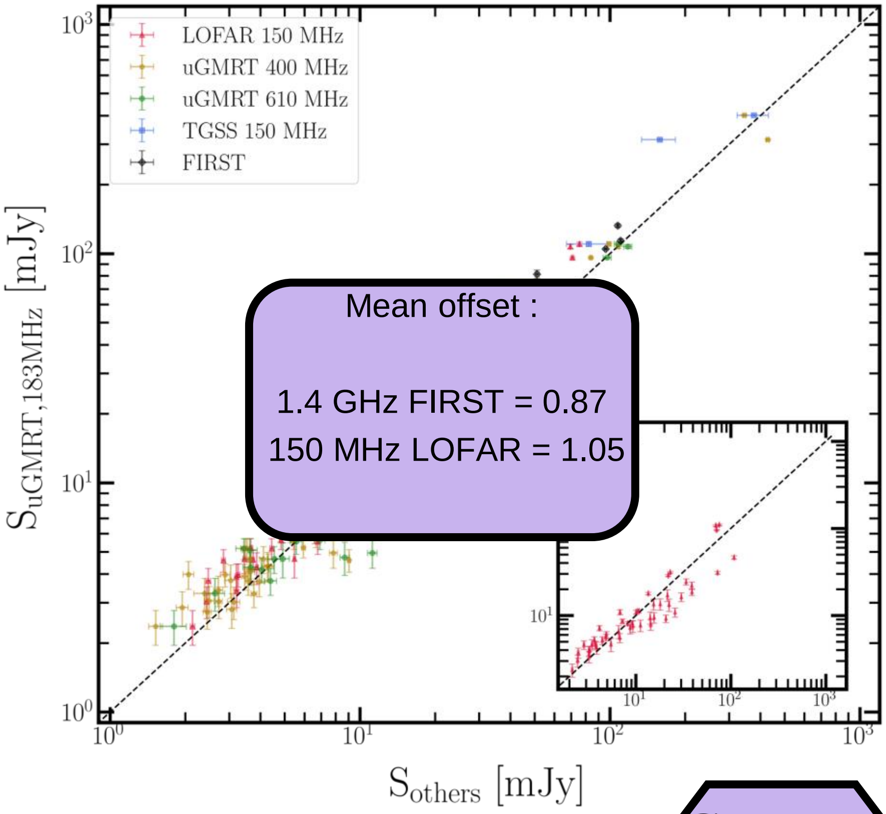

Mean offset :

1.4 GHz FIRST = 0.87

150 MHz LOFAR = 1.05

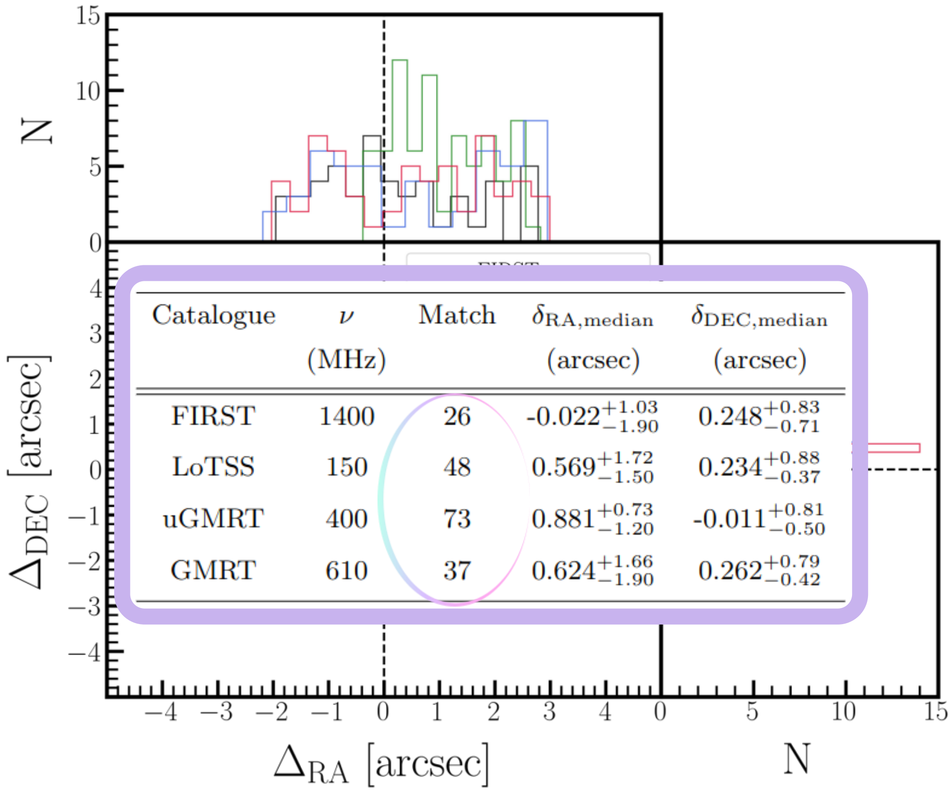

Catalogue	ν (MHz)	Match	$\delta_{\mathrm{RA,median}}$ (arcsec)	$\delta_{\mathrm{DEC,median}}$ (arcsec)
FIRST	1400	26	$-0.022^{+1.03}_{-1.90}$	$0.248^{+0.83}_{-0.71}$
LoTSS	150	48	$0.569^{+1.72}_{-1.50}$	$0.234^{+0.88}_{-0.37}$
uGMRT	400	73	$0.881^{+0.73}_{-1.20}$	$-0.011^{+0.81}_{-0.50}$
GMRT	610	37	$0.624^{+1.66}_{-1.90}$	$0.262^{+0.79}_{-0.42}$

$$\mathbf{S}_\nu \propto \nu^\alpha$$

Sagar et al., (In prep.)

Spectral Index

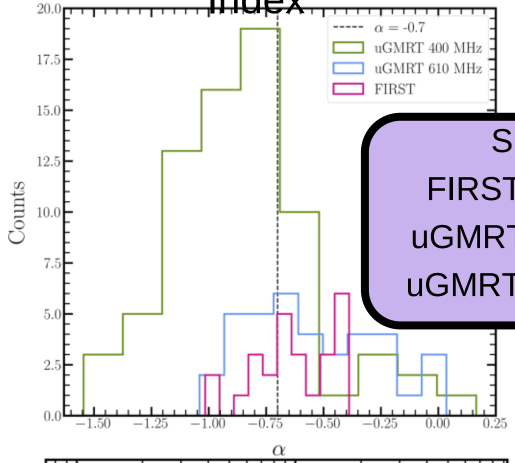

Spectral Index
FIRST 1.4 GHz = -0.63
uGMRT 400 MHz = - 0.87
uGMRT 610 MHz = - 0.57

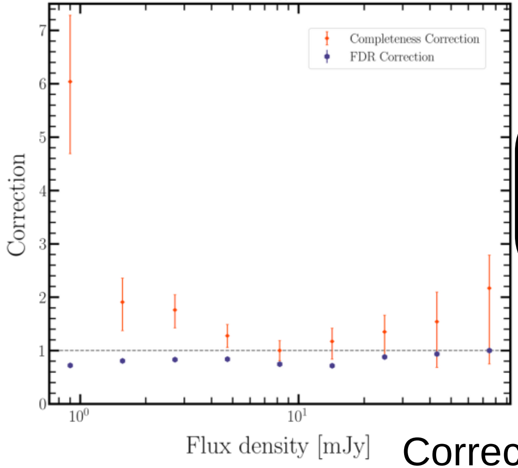

$$f_{real,i} = \frac{N_{catalog,i} - N_{inv,i}}{N_{catalog,i}}$$

$$Correction_{,i} = \frac{N_{injected,i}}{N_{recovered,i}}$$

Hale et al. 2019

Correction for biases

Source Counts

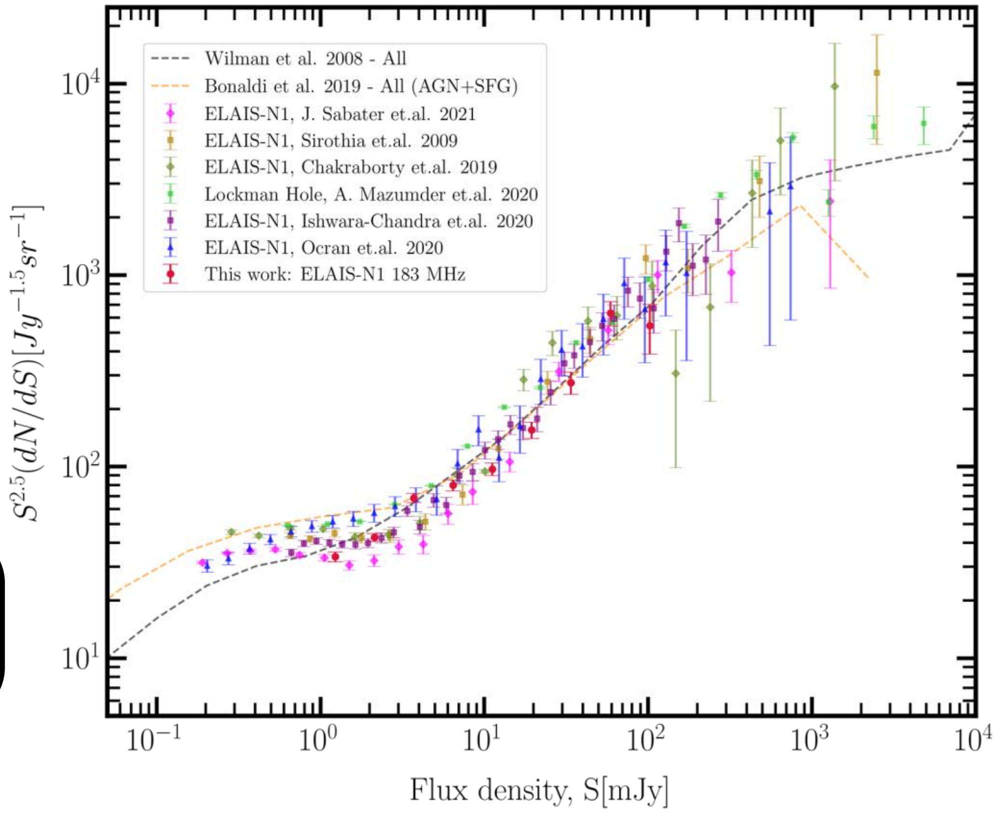

Sagar et al., (In prep.)

Angular Power Spectrum : BAND-3

416MHz

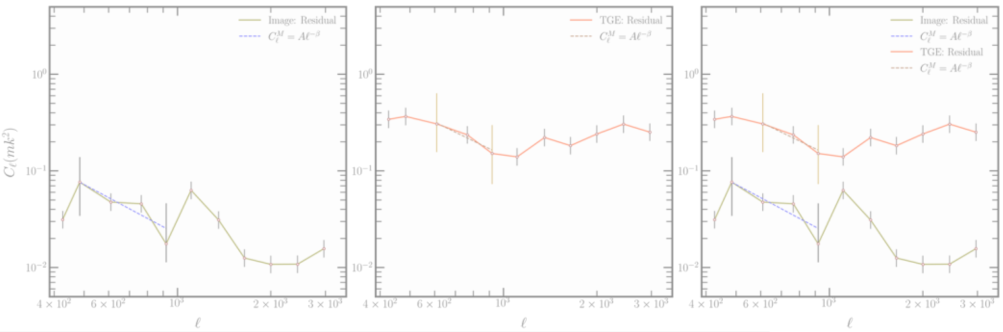

ν (MHz)	i-APS			t-APS		
	A (mK^2)	β	$\ell_{min} - \ell_{max}$	A (mK^2)	β	$\ell_{min} - \ell_{max}$
316	1.487 ± 0.111	2.102 ± 0.331	$419 - 918$	1.087 ± 0.029	1.779 ± 0.120	$751 - 1114$
350	0.540 ± 0.026	2.961 ± 0.325	$400 - 621$	0.472 ± 0.039	1.888 ± 0.464	$621 - 755$
383	0.382 ± 0.018	2.726 ± 0.189	$507 - 909$	0.174 ± 0.028	2.353 ± 0.366	$620 - 909$
416	0.114 ± 0.023	2.108 ± 0.557	$483 - 919$	0.144 ± 0.020	1.562 ± 0.341	$609 - 919$
450	0.021 ± 0.005	2.920 ± 0.594	$514 - 919$	0.328 ± 0.019	1.574 ± 0.179	$1105 - 1993$
483	0.332 ± 0.001	3.016 ± 0.334	$481 - 730$	0.471 ± 0.009	1.935 ± 0.071	1121 – 200[illegible]

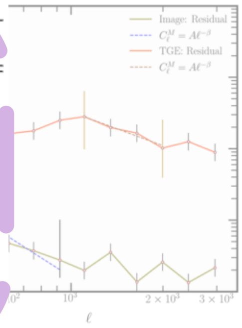

483MHz

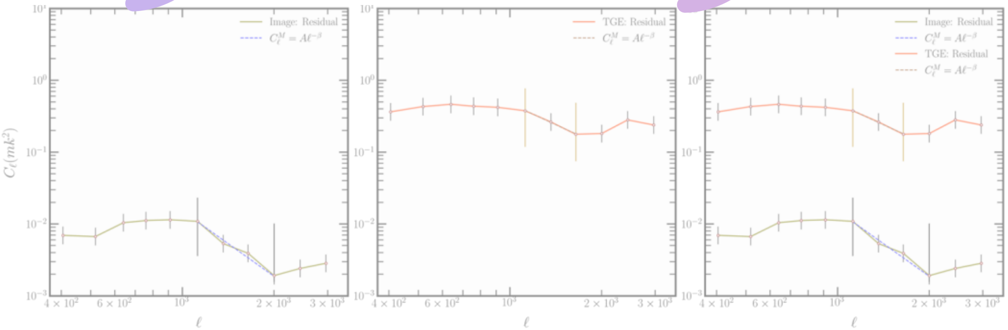

Sagar et al., (In prep)

Upper limit on 21-cm signal with other telescopes at High - z

Reionization epoch (z > 6)

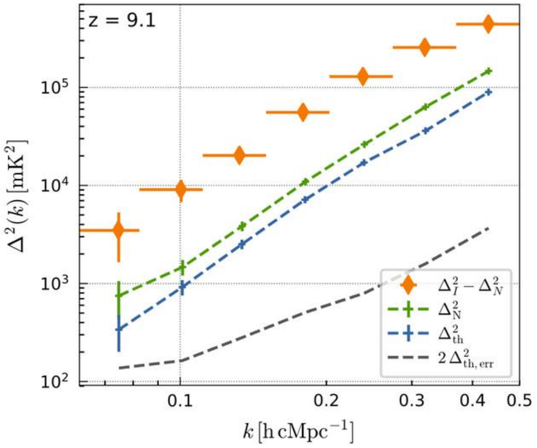

LOFAR

z ≈ 9.1

Mertens et al., 2020

HERA Phase I

Abdurashidova et al., 2022

Band 1 (z = 10.4) and Band 2 (z = 7.9)

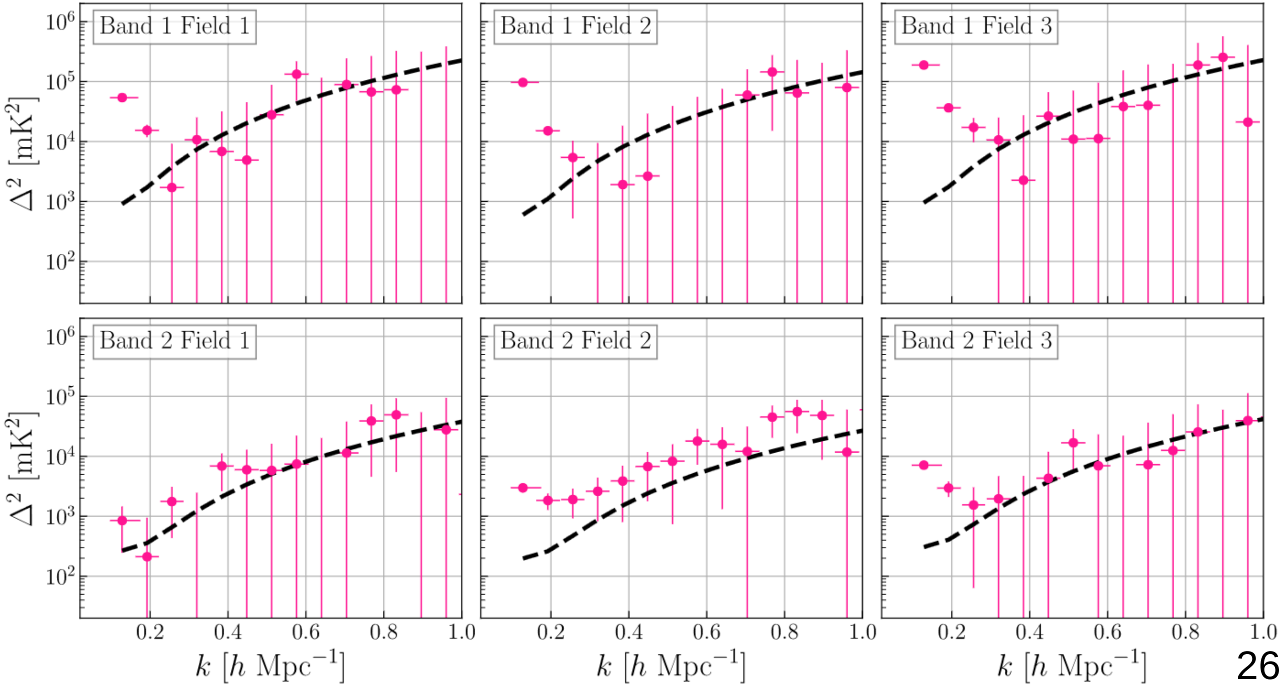

Estimated PS using Polynomial Fitting (order n = 3) from point source subtracted data

Image area = central 2.8x2.8 degrees

Bandwidth ~ 14.6 MHz

Observation Time ~ 8 hour

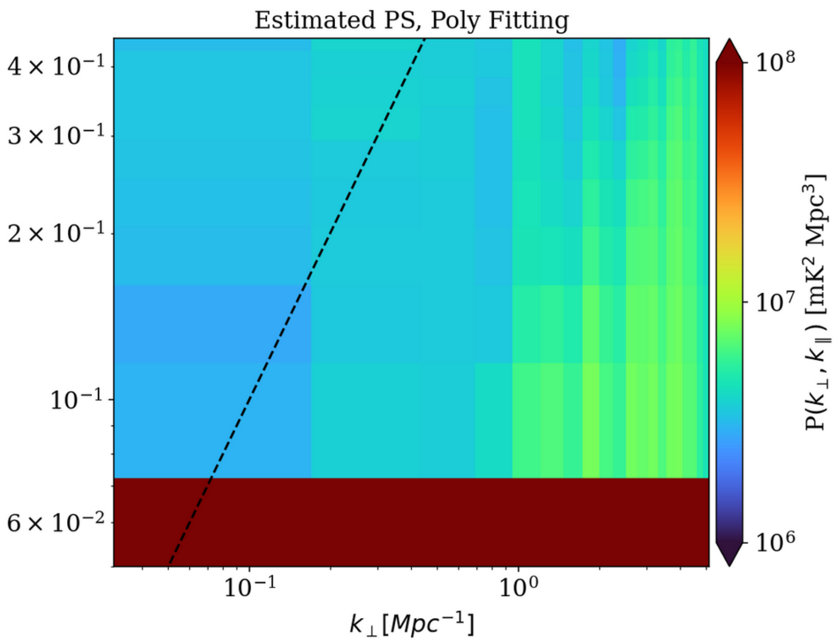

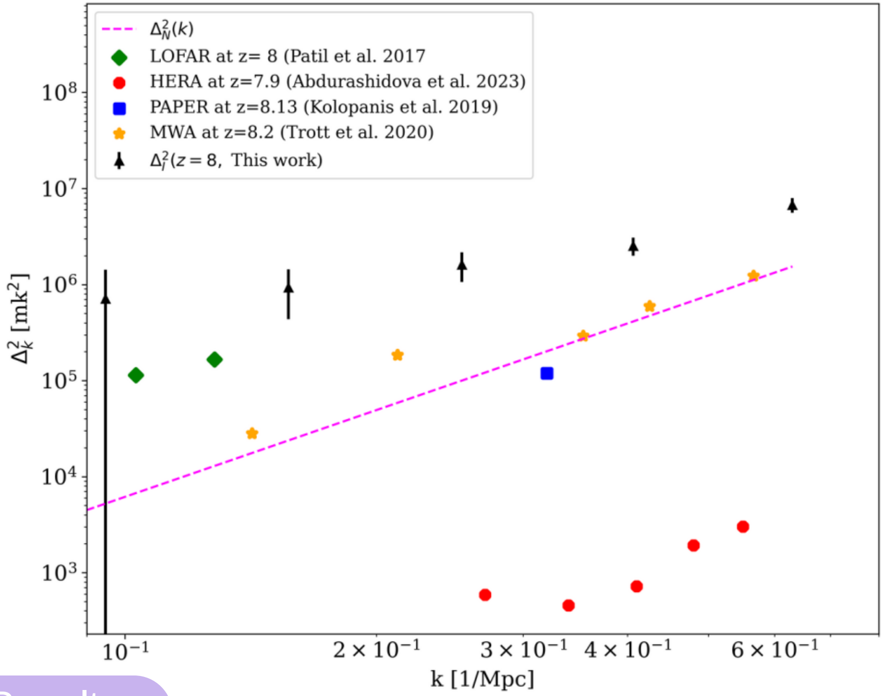

Initial Results

Estimated PS for point source and residual data

Image area = central 2.8x2.8 degrees

Bandwidth ~ 6.6 MHz

Observation Time ~ 8 hour

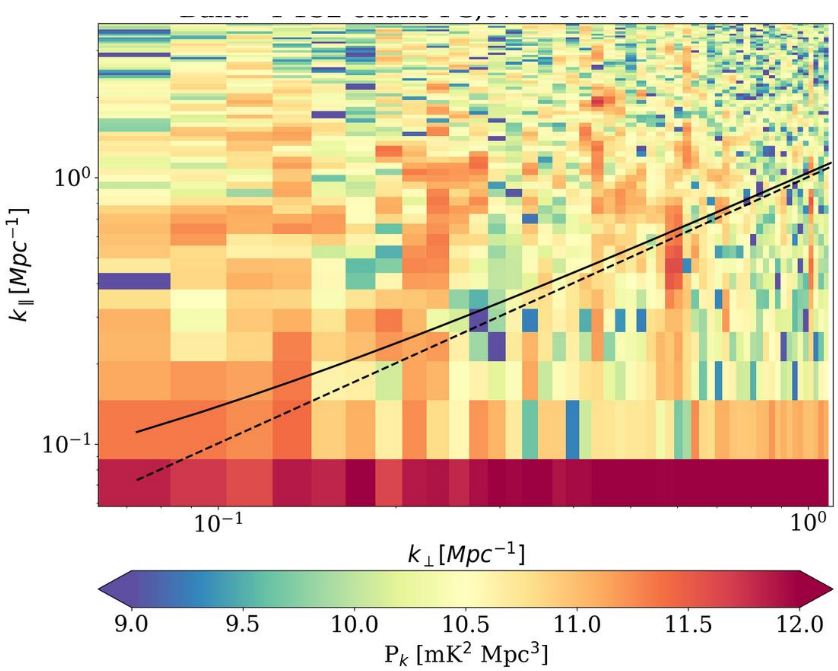

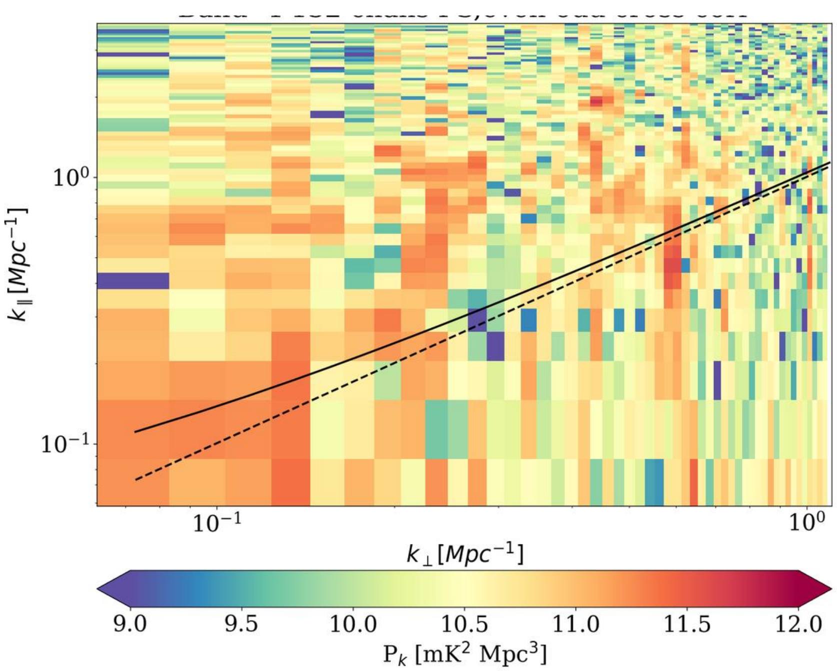

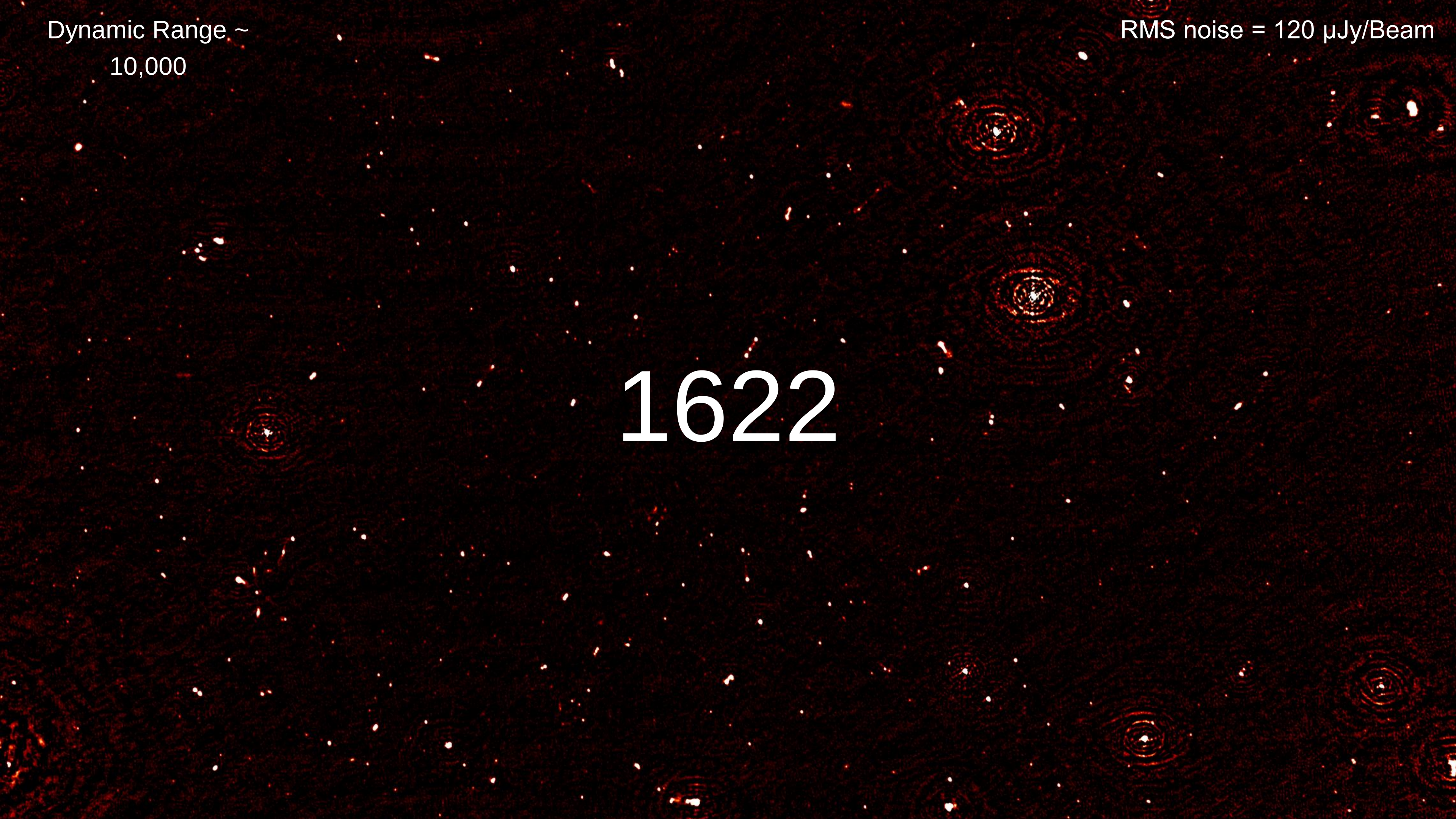
Dynamic Range ~
10,000
RMS noise = 120 μJy/Beam
1622

Understanding Systematics:

Development of 21cmE2E Pipeline for DI and DD calibration Errors from visual observation of 2D and 1D PS

Flowchart: Observational Pipeline - 21cmE2E

- In A. Mazumder et al. 2022, they have developed the 21cmE2E pipeline to simulate interferometric observation.

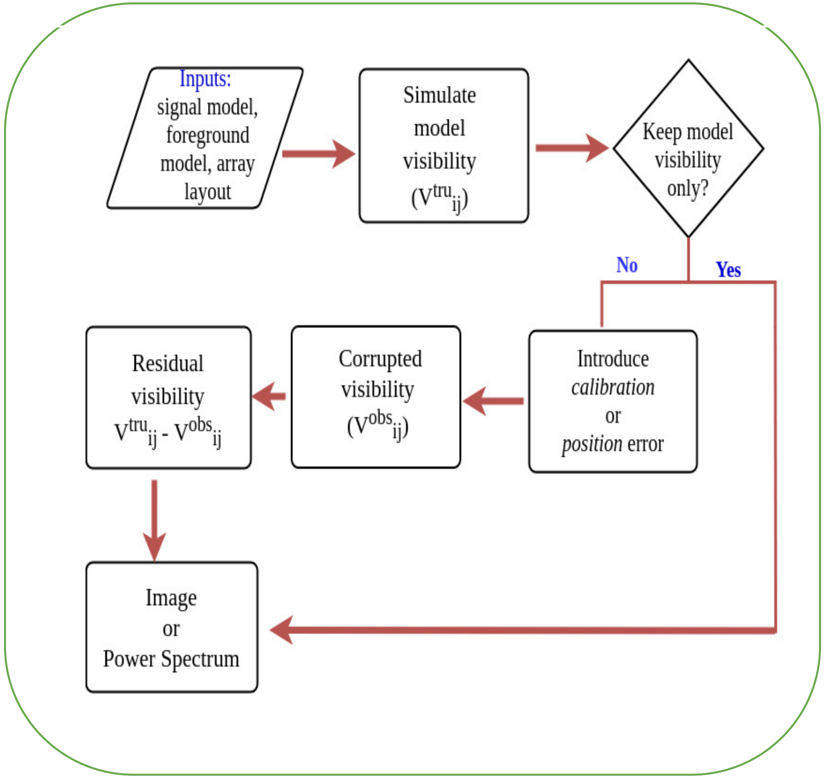

(A Mazumder et al. 2022)

Simulation inputs for the Synthetic Observation

21cm Signal

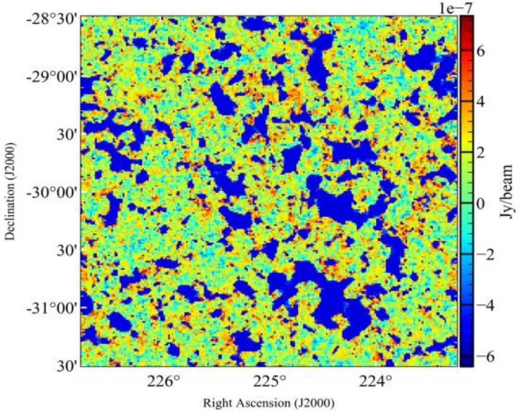

Global sky model

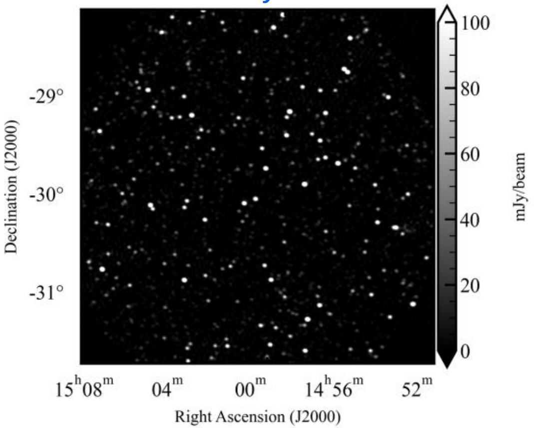

Telescope Model

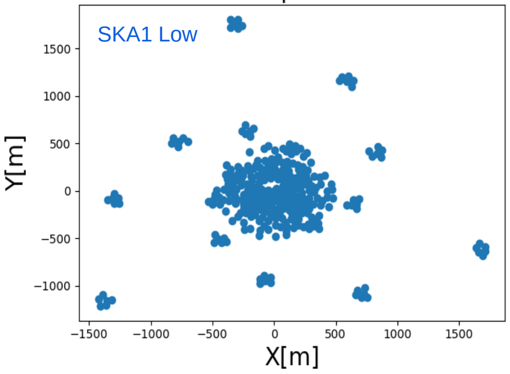

Parameter	Value
Central Frequency	142 MHz (z~9)
Bandwidth	8 MHz
Number of frequency channels	64
Field of view	4°
Number of array elements:	
SKA1-Low Core	296
Maximum baseline (m):	2000
Synthesised beam (arcmin):	2.5

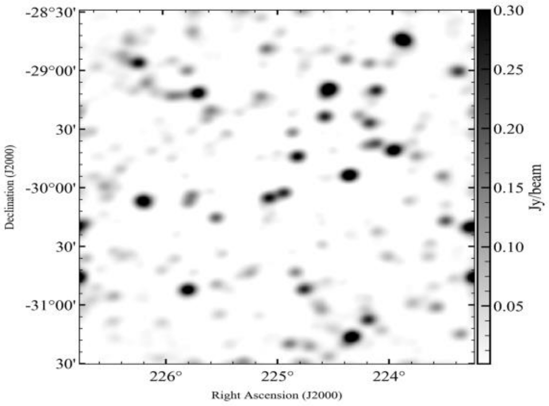

Utility of this Observation Pipeline for Various Scientific Case Studies

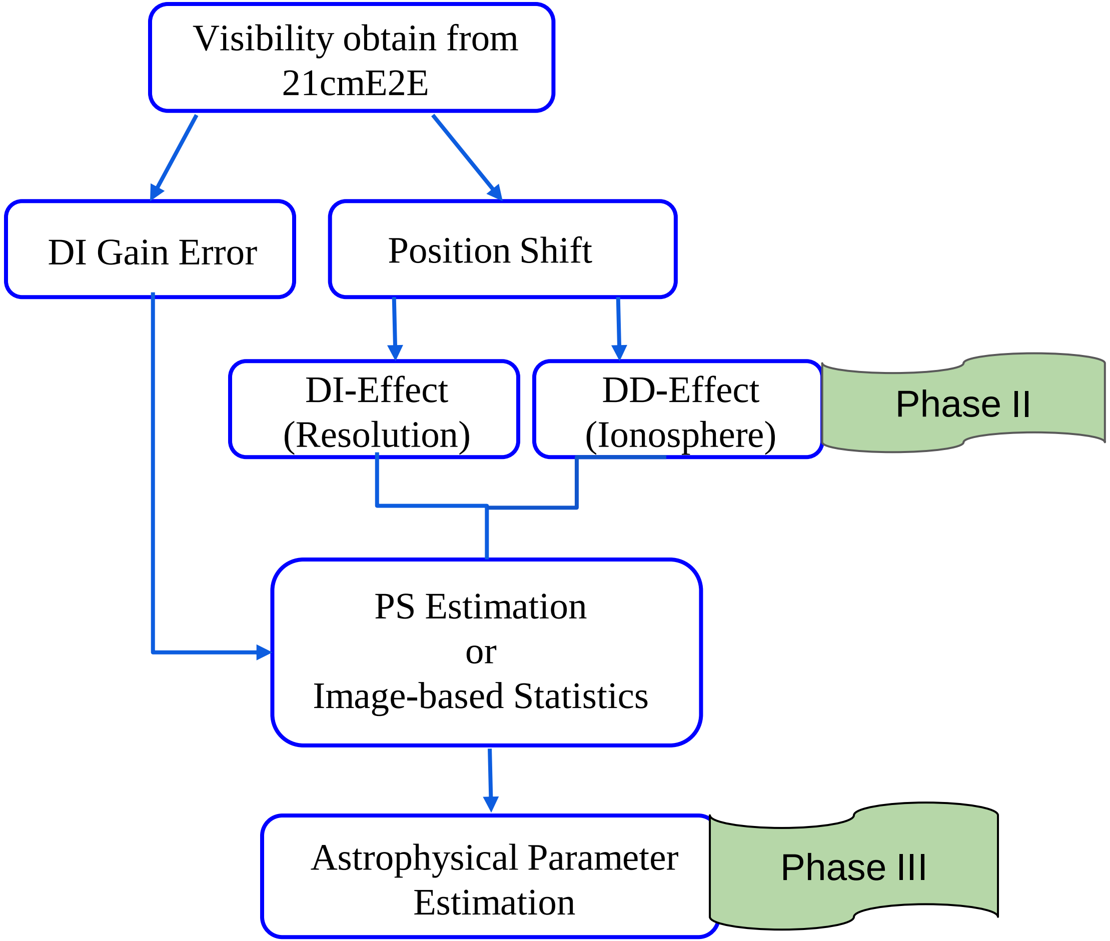

Power Spectrum Estimation : DI Gain Calibration Error

- Power spectrum analysis - Spherical averaged PS follows signal power if residual calibration error is > 0.1% is exceeds signal power significantly for greater error

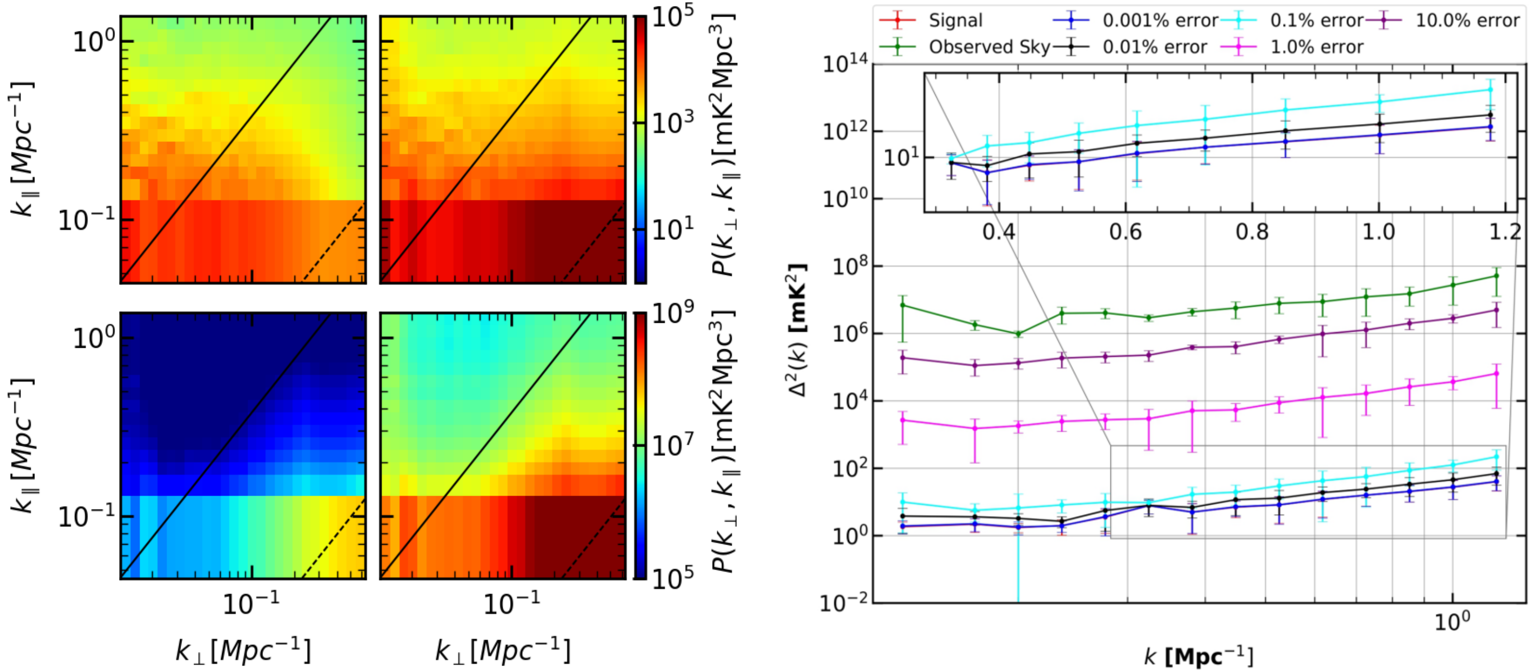

Mazumder et al. 2022

Effect of ionosphere on Radio Observation

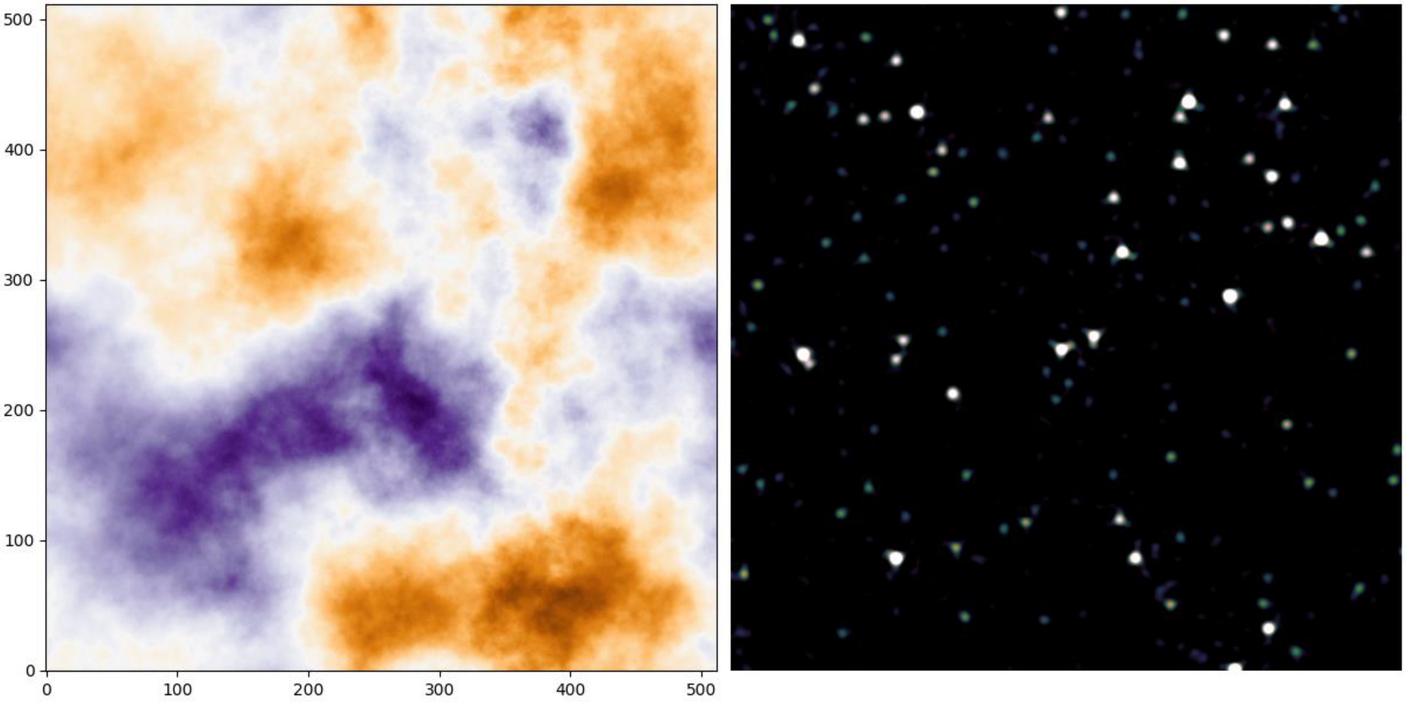

Animation of source offset in presence of Kolmogorov turbulence

Pal et al., in prep

Ionosphere activity on Murchison Radio-astronomy Observatory location

- 4 main ionosphere activity types categorized at MRO location based on apparent position shift and spatial structure.

  Jordan et. al. 2017

- Galactic and Extragalactic All-Sky MWA Survey shows the the angular scales of the ionospheric structure are typically 100 km.

  Helmboldt & Hurley-Walker et. al., 2020

- Ionospheric activity - simulated extremely quiet to active condition.

- **Median ionospheric offset (MIO)** - quantifying metric of ionospheric activity.

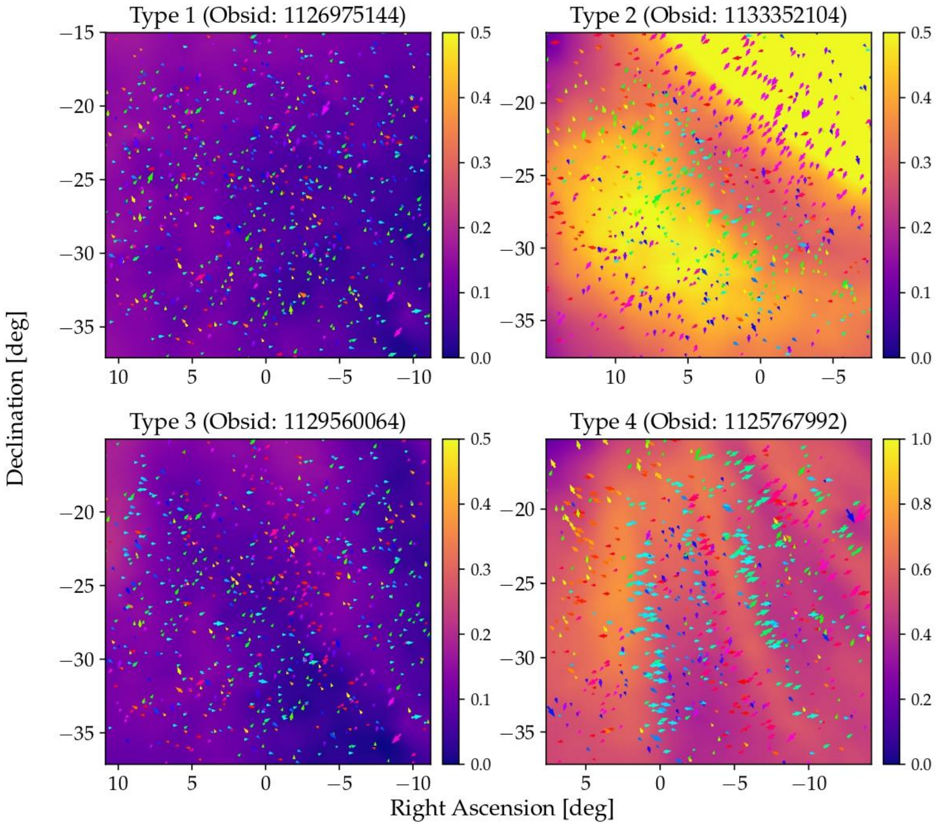

Image credit: Jordan et. al., 2017

Ionospheric Models : Refractive Shift

- Apparent position shift added to each source along RA direction using Gaussian distribution.
- The ionospheric activities are simulated are comparable in real MWA observation based on Jordan et al. 2017.
- Apparent position offset of the cosmic sources :

$$\vec{\nabla} TEC = 1.20 \times 10^{-4} \left(\frac{f}{100 MHz} \right)^2 \left(\frac{\vec{\delta}\theta}{1''} \right) TECU km^{-1}$$

Helmboldt & Hurley-Walker et al., 2020

- For each timestamp of 2 minutes, the local structure remains the same and consistent.

Wayth et al. 2015

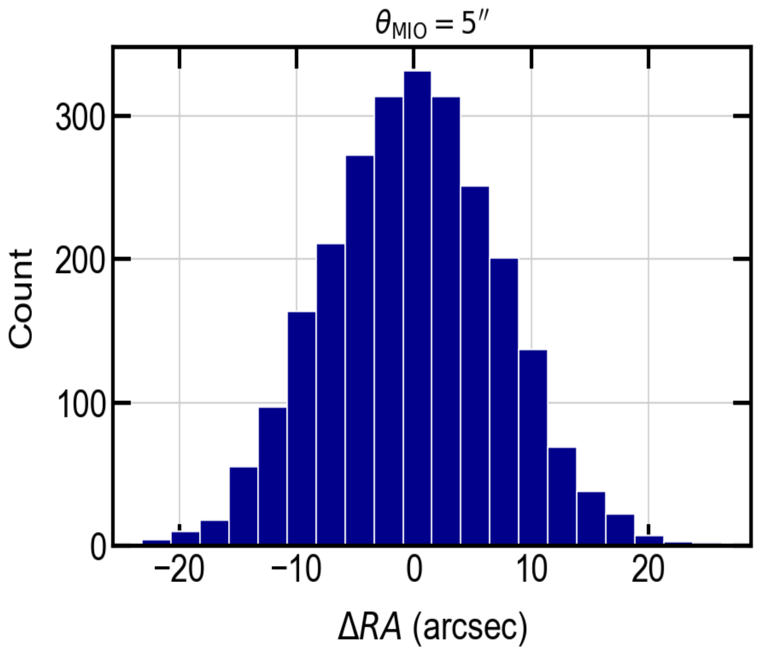

Pal et al., in prep

Ionospheric Models: Kolmogorov Turbulence Model

- The power spectrum of the spatial phase function is

$$\left|\Phi(\vec{k})\right|^2 \propto \left[k^2 + \left(\frac{1}{L_0}\right)^2\right]^{-\alpha/2} \exp\left(-\frac{k^2}{2/l_0^2}\right); 1/L_0 \ll k \ll 1/l_0$$

- Time evolving phase screen -

$$\Phi_{new}(\vec{k}) = \Phi_{old}(\vec{k})exp\left(2\pi i\vec{k}N_s/N\right)$$

Glindemann et al., 2007

- For each timestamp of 2 minutes, the local structure remains the same and consistent.

Wayth et al. 2015

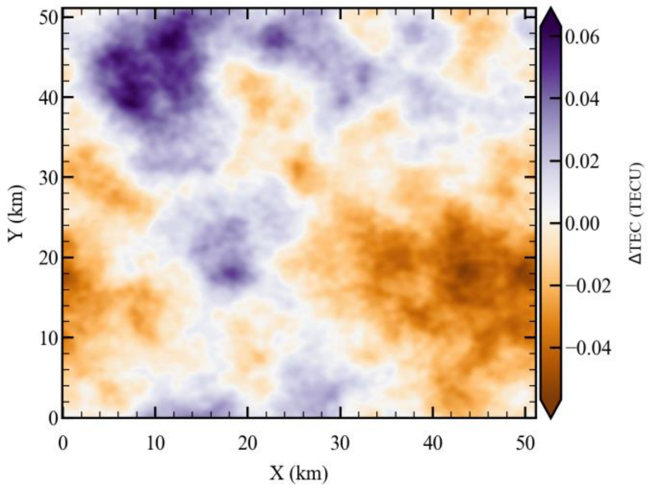

Pal et al., in prep

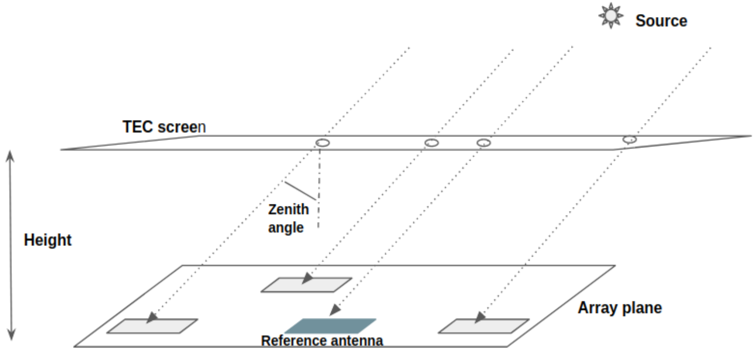

Schematics representation of Earth's Ionosphere
Image Credit: Chage et al., 2021

Power Spectrum Estimation : Refractive Shift

- Foreground leakage to the EoR window with increasing source displacement.

- Power spectrum analysis - Spherical averaged PS follows signal power if sources are displaced by ionospheric median offset of 0.2 arcsec , greater error lead to higher amplitude of residual power wrt signal power.

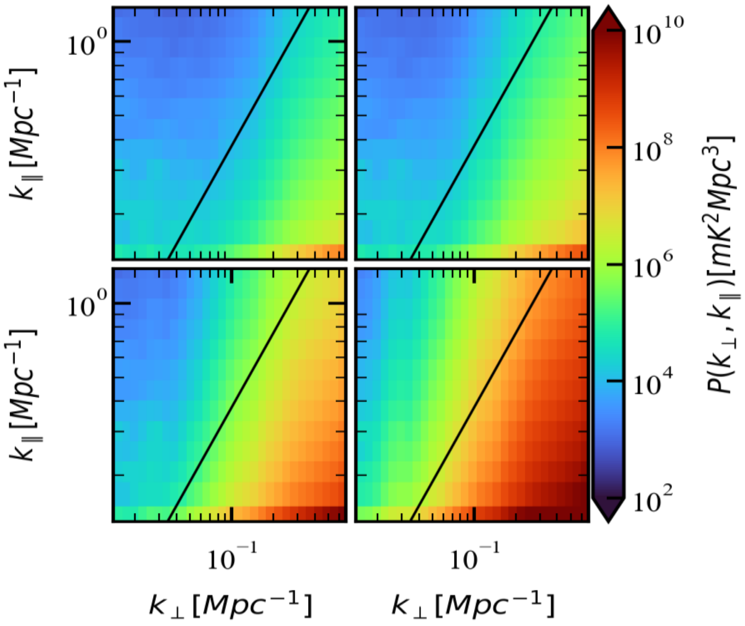

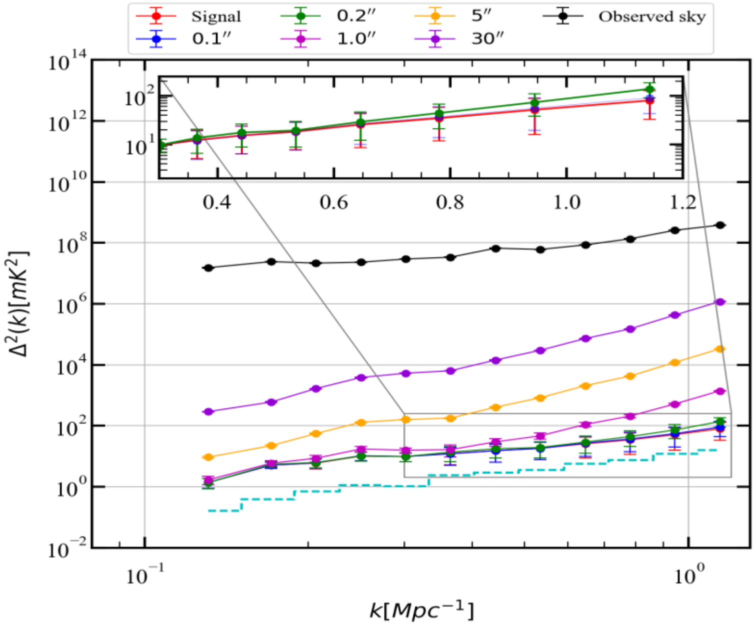

Pal et al., in prep

Power Spectrum Estimation : Kolmogorov Turbulence

- Foreground leakage to the EoR window with increasing source displacement.

- Power spectrum analysis - Spherical averaged PS follows signal power if sources are displaced by ionospheric median offset of 0.1 arcsec , greater error lead to higher amplitude of residual power wrt signal power.

- Beyond the 0.1 arcsec, residual power surpasses the target signal PS across all accessible k-modes

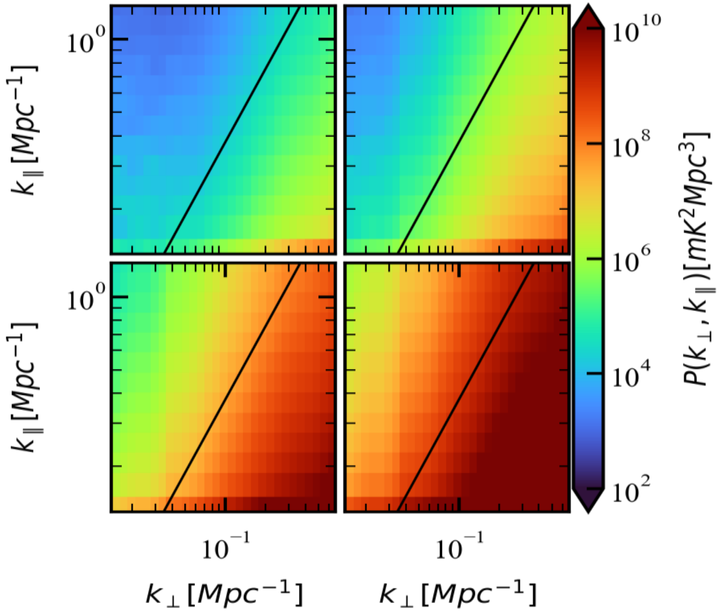

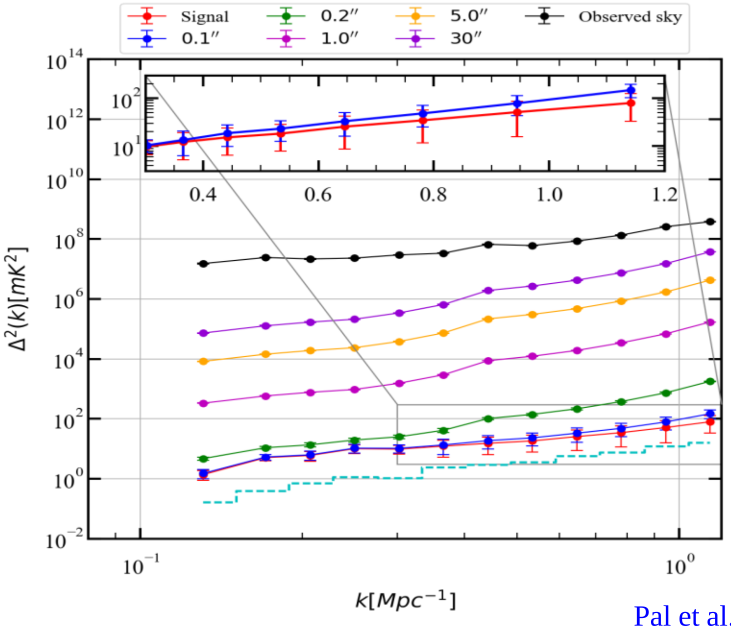

Pal et al., in prep

Summary/Takeaways

- We assess the effects of different ionospheric conditions ranging from quiet to extreme conditions.
- We observed that depending on the specific type of disturbance induced, ionospheric corruption significantly affects the recovery of the target signal in the k-scales .
- For the case of a time-varying phase offset, if sources are shifted by up to $0.2''$ on average, the HI power spectrum is recoverable.
- The most realistic turbulent condition generated using Kolmogorov's statistics shows that beyond $\sim 0.1''$, residual power is too high for 21 cm signal recovery.
- These results indicate that understanding the ionospheric conditions during observation runs for EoR science is essential since such unaccounted effects, even to first order, can adversely affect signal recovery.

Extracting the 21-cm Power Spectrum and associated parameters With DI Calibrated Gain Error

Training Data sets

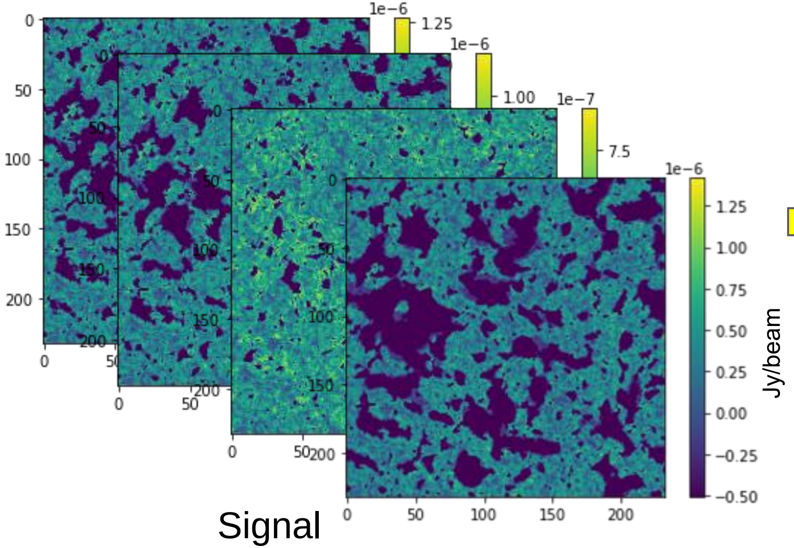

Signal

Telescope Model
(SKA1_Low)

21cmE2E pipeline

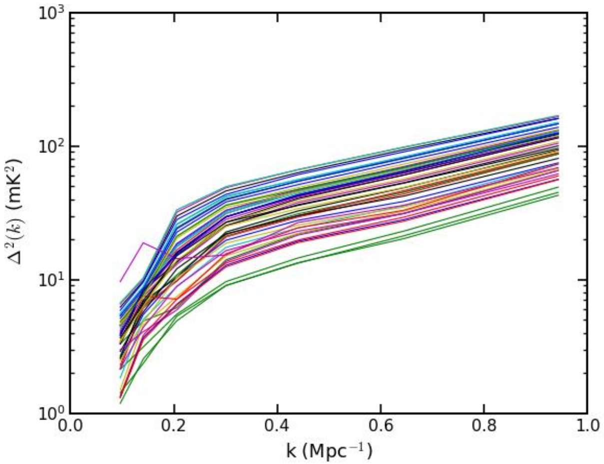

Fig : 300 datasets of the HI Power spectrums for the training.

Parameters Ranges

R_{mfp} = 10 Mpc to 60 Mpc
ζ = 10 to 60
T_{vir} = 4.5 to 6.0 (in dex)
(H.Shimabukuro et al. 2017)

Tripathi A et al. (in prep)

Emulating Power Spectrum and Parameter Extraction

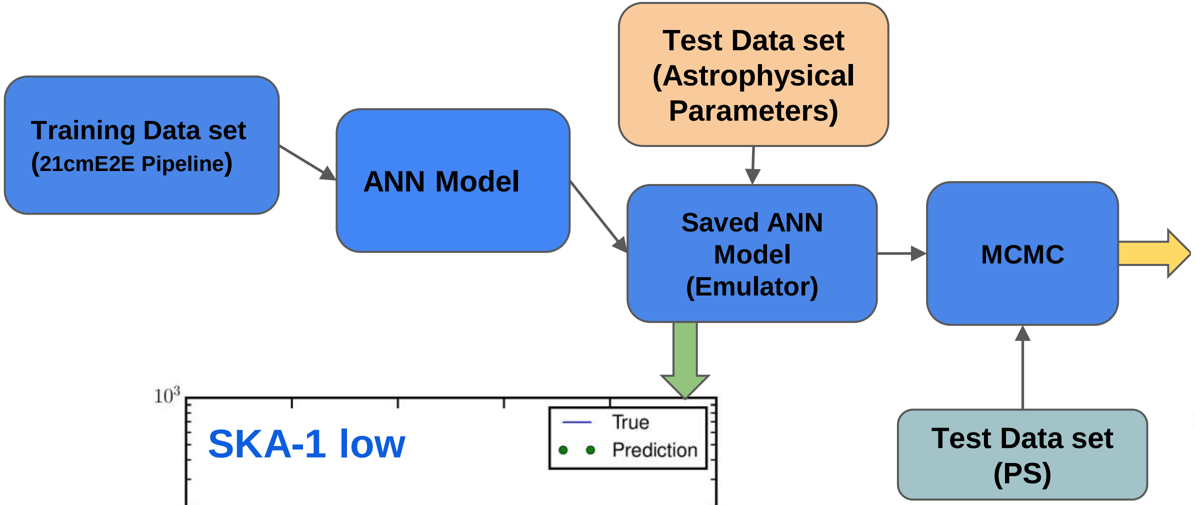

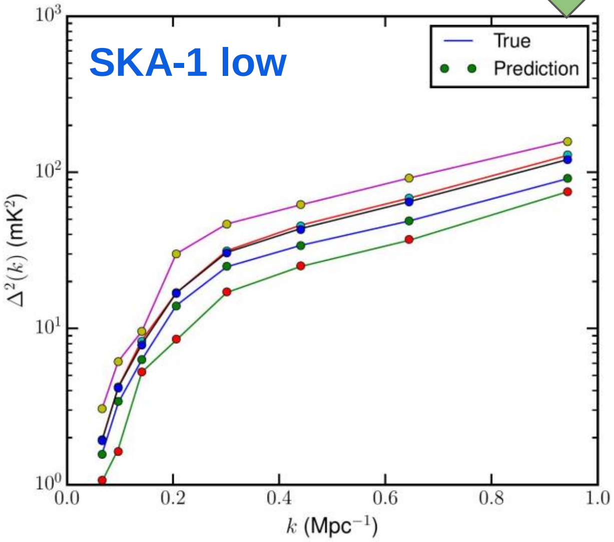

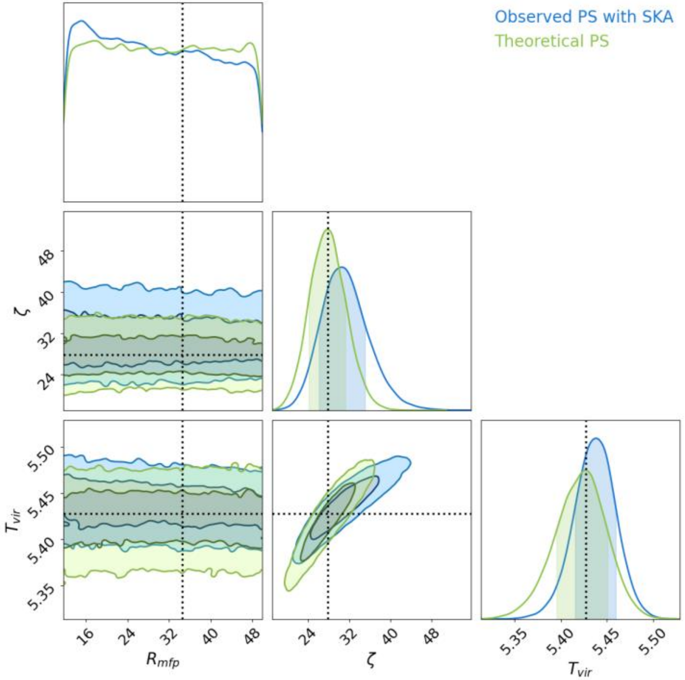

Parameters	True Value	Observed PS with SKA1 low (MCMC)
R_{mfp}	34.67	–
ζ	27.92	$31.6^{+5.2}_{-4.0}$
T_{vir}	5.428	$5.439^{+0.021}_{-0.021}$

Tripathi A et al. (2024, in prep)

MCMC Prediction for different Astrophysical Conditions

	Parameters	True Value	Observed PS with SKA1 low (MCMC)
PS1	R_{mfp}	34.67	–
	ζ	27.92	$31.6^{+5.2}_{-4.0}$
	T_{vir}	5.428	$5.439^{+0.021}_{-0.021}$
PS2	R_{mfp}	12.2	$20.0^{+14.1}_{-8.2}$
	ζ	18.42	$20.0^{+4.9}_{-3.9}$
	T_{vir}	4.738	$4.764^{+0.034}_{-0.047}$
PS3	R_{mfp}	44.33	–
	ζ	57.42	$59.8^{+0.0}_{-9.3}$
	T_{vir}	5.928	$5.926^{+0.013}_{-0.013}$

Tripathi A et al. (in prep)

- In all cases, the ANN-based MCMC model's inferred ionizing efficiency (**ζ**) and T_{vir} closely match true values, but R_{mfp} is highly degenerate.
- Indicates model robustness for further study of calibrated Gain error and position error.

SKA1-Low with Calibrated Gain Error

$$V_{ij}^{m} = g_i(t) g_j^*(t) V_{ij}^{t}$$

Gain error
$$\begin{cases} g_i = (a_i + \delta a_i)\exp(-i(\phi_i + \delta\phi_i)) \\ g_i = (1 + \delta a_i)\exp(-\delta\phi_i) \end{cases}$$

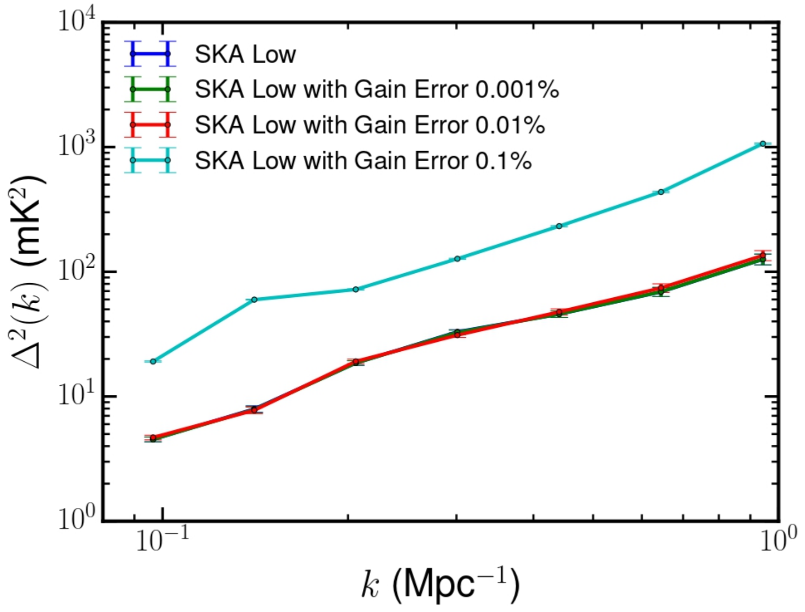

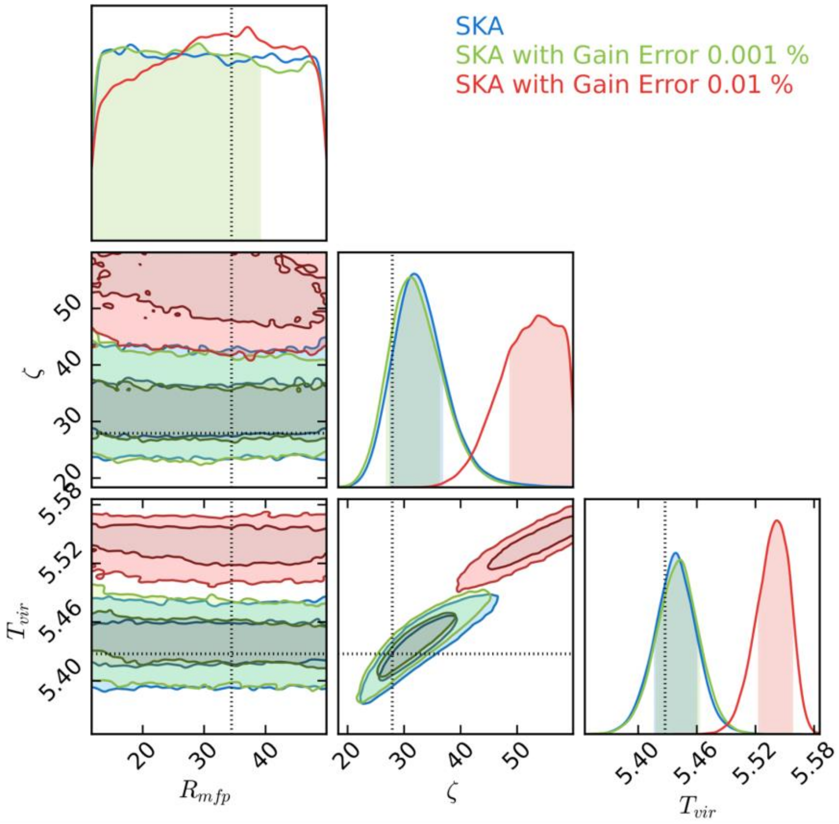

Tripathi A et al. (in prep)

Summary/Takeaways

- Inherent bias in the 21cm power spectra due to the effect of the PSF of an radio interferometer.
- If the gain error exceeds 0.001% for both interferometers, our derived astrophysical parameters will be biased due to the presence of gain error.
- Position errors exceeding 0.05 arcsec will bias the astrophysical parameters.
- This pipeline can be extended to study effects of chromatic primary beam, radio frequency interferences, foregrounds with spectral features.